Check for updates

Geophysical Research Letters

RESEARCH LETTER
10.1029/2023GL106433

Key Points:

- Outgoing longwave radiation increases with CO_2 concentration in the Arctic and tropics in certain circumstances, in addition to commonly occurring in Antarctica
- In polar regions, negative CO_2 forcing arises from stratospheric temperature inversions, while near-surface inversions have a small effect
- CO_2 forcing can be negative in other regions when high clouds block the tropospheric emission, leaving the stratospheric contribution

Correspondence to:

Y.-T. Chen,
yan-ting.chen@mail.mcgill.ca

Citation:

Chen, Y.-T., Merlis, T. M., & Huang, Y. (2024). The cause of negative CO_2 forcing at the top-of-atmosphere: The role of stratospheric versus tropospheric temperature inversions. *Geophysical Research Letters*, *51*, e2023GL106433. https://doi.org/10.1029/2023GL106433

Received 19 SEP 2023
Accepted 3 DEC 2023

© 2024 The Authors.
This is an open access article under the terms of the Creative Commons Attribution-NonCommercial License, which permits use, distribution and reproduction in any medium, provided the original work is properly cited and is not used for commercial purposes.

The Cause of Negative CO_2 Forcing at the Top-Of-Atmosphere: The Role of Stratospheric Versus Tropospheric Temperature Inversions

Yan-Ting Chen[1], Timothy M. Merlis[2], and Yi Huang[1]

[1]Department of Atmospheric and Oceanic Sciences, McGill University, Montreal, QC, Canada, [2]Program in Atmospheric and Oceanic Sciences, Princeton University, Princeton, NJ, USA

Abstract Increasing carbon dioxide (CO_2) in the atmosphere usually reduces Earth's outgoing longwave radiation (OLR). The unusual case of Antarctica, where CO_2 enhances OLR and implies a negative forcing, has previously been explained by the strong near-surface inversion or extremely low surface temperature. However, negative forcing can occasionally be found in the Arctic and tropics where neither of these explanations applies. Here, we examine the changes in infrared opacity from CO_2 doubling in these low or negative forcing climate states, which shows the predominant role of the stratospheric contribution to the broadband forcing. Negative forcing in today's climate demands a combination of strong negative forcing caused by a steep stratospheric temperature inversion and a weaker positive forcing in the atmospheric window, which can be caused by a low surface temperature or a strong high cloud masking effect. Contrary to conventional wisdom, the near-surface inversion has little impact on the forcing.

Plain Language Summary Carbon dioxide (CO_2), as an important greenhouse gas, is known to reduce the Earth's longwave emission, provoking a positive forcing that increases the net flow of energy into the Earth system. In this study, we discuss the cause of negative forcing, where CO_2 increases longwave emission that happens most commonly in Antarctica and in some rare conditions in the Arctic and tropics. In contrast to conventional arguments that a near-surface temperature increase with altitude is key to a negative CO_2 forcing, we show that the stratospheric temperature and, in the tropics, clouds play a more important role. The results are based on temperature modification experiments and an analysis of the vertical structure of atmospheric emission changes. While a negative forcing does not mean the surface would cool since there are other important adjustments involved in the re-establishment of energy balance, the results show the values of resolving the spectral dimension of radiation to quantify the radiative sensitivity to the near-surface and stratosphere temperature structure.

1. Introduction

It is known that increasing carbon dioxide (CO_2) concentration enhances the greenhouse effect and results in positive longwave radiative forcing at the top-of-atmosphere (TOA), leading to an increase in Earth's radiation budget. While this is true in general, it has also been shown that the CO_2 forcing can enhance longwave emission-to-space in Antarctica, which is a negative TOA forcing. Such phenomenon is found in radiative transfer calculations (Chen et al., 2023; Flanner et al., 2018; Freese & Cronin, 2021; Jeevanjee et al., 2021; Zhang & Huang, 2014) and climate models (Huang et al., 2016; Schmithüsen et al., 2015; K. L. Smith et al., 2018), with support from observations (Schmithüsen et al., 2015; Sejas et al., 2018). Although a negative TOA forcing there might not translate to surface cooling (K. L. Smith et al., 2018; Freese & Cronin, 2021) and there are other forcing metrics, such as effective radiative forcing, that could be more predictive of surface temperature response (Myhre et al., 2013), understanding what distinguishes the radiative forcing in Antarctica from other parts of the climate helps improve theoretical understanding of the radiative forcing.

Existing understandings from spectral radiative transfer properties shed light on negative TOA forcing from increased CO_2. This can result from the non-monotonic vertical temperature structure. In a non-scattering atmosphere, the radiance at the TOA ($z = \infty$) at a wavenumber ν can be written as:

$$I_\nu(\infty) = B_\nu(0)\,\mathrm{Tr}_\nu(0) + \int_0^\infty B_\nu(z)\,W_\nu(z)\,dz, \tag{1}$$

$$\mathrm{Tr}_\nu(z) \equiv e^{-\tau_\nu(z)}, \tag{2}$$

$$W_\nu(z) \equiv \frac{d\mathrm{Tr}_\nu(z)}{dz}, \tag{3}$$

where I_ν is the monochromatic radiance, $B_\nu(z)$ is the thermal emission of the layer at the height z, $\mathrm{Tr}_\nu(z)$ is the transmissivity between z and the TOA, $\tau_\nu(z)$ is the optical depth between the TOA and z that monotonically increases from the TOA to the surface, and $W_\nu(z)$, the weighting function, is the derivative of the transmission function with height.

As CO_2 increases, the altitude of the weighting function peak, or the so-called emission layer where $\tau_\nu(z) = 1$, shifts to a higher level (e.g., Huang & Bani Shahabadi, 2014). When collocated with a temperature inversion, the elevated emission layer enhances emission-to-space from the warmer air (as opposed to having colder air above, as is typical in the troposphere) and therefore leads to a negative TOA forcing. Such negative forcing in monochromatic radiance has been identified in individual wavelengths where the emission layer shifts within either stratospheric (Huang & Bani Shahabadi, 2014) or near-surface (Flanner et al., 2018; Sejas et al., 2018) temperature inversion. As the gas absorption properties vary spectrally, the behavior at a single wavelength does not determine the broadband results. Antarctica, interestingly, is a region where the negative forcing remains after spectral integration.

From a simplified, broadband perspective, Schmithüsen et al. (2015) and K. L. Smith et al. (2018) approximated the TOA forcing with a two-level model. Assuming an effective emission temperature of the atmosphere and the Earth's surface is a blackbody, the outgoing longwave radiation (OLR) at the TOA is expressed as:

$$\mathrm{OLR} = (1 - \epsilon_{ATM})\sigma T_{SFC}^4 + \epsilon_{ATM}\sigma T_{ATM}^4, \tag{4}$$

where ϵ_{ATM} is the broadband emissivity of the atmosphere and equals broadband $1 - \mathrm{Tr}(0)$ in Equation 1. As higher CO_2 concentration increases ϵ_{ATM}, the dependency of instantaneous forcing is then:

$$\frac{\partial \mathrm{OLR}}{\partial \epsilon_{ATM}} = \sigma\left(T_{ATM}^4 - T_{SFC}^4\right). \tag{5}$$

From this equation, the sign of the forcing is determined by the temperature contrast between the surface and the atmosphere: when $T_{ATM} > T_{SFC}$, OLR increases as CO_2 increases ϵ_{ATM}. Schmithüsen et al. (2015) and K. L. Smith et al. (2018) concluded that a stratosphere warmer than the surface results in negative CO_2 forcing. However, neither of these works quantifies T_{ATM} in Equation 5. There are also times like June in Antarctica that have a portion of the stratosphere that is warmer than T_{SFC}, yet have positive CO_2 forcing. Although Schmithüsen et al. (2015) mentioned that the emission around the CO_2 absorption band originates mostly from the stratosphere, the two-level model is not appropriate for this spectral region: in the bands with strongly absorbing gases, ϵ_{ATM} reaches unity and no longer increases with additional CO_2. This suggests that the forcing does not follow the form of Equation 5 and raises questions about its utility in explaining the negative CO_2 forcing. Using different approaches, Jeevanjee et al. (2021) and Chen et al. (2023) reproduced Antarctica's negative CO_2 forcing by contrasts in T_{SFC} and a well-defined stratospheric temperature as T_{ATM}, but both of these adopted parameters to approximate the global CO_2 forcing patterns and did not isolate the forcing results from inversions. The role of stratospheric and tropospheric inversions, therefore, remains unclear.

Negative TOA forcing of CO_2 increase also happens outside of Antarctica. The Arctic sometimes exhibits strong negative CO_2 forcing (Figure 1a). This phenomenon even occurs in the tropics and mid-latitudes for instances of strong longwave cloud radiative effects (CRE), when the all-sky OLR is much lower than the clear-sky OLR. Although such extreme events are smoothed out in the long-term average, these occasions of negative forcing are worth documenting and suggest that there are other factors that can sharply modify the forcing, in addition to simple surface temperature-based or stratospheric temperature-based arguments.

This study explores the causes of negative TOA CO_2 forcing, which happens in about 3% of daily mean samples globally, with focuses on the polar regions and tropics. The distinct climates there will generalize the current understanding of how the temperature structure and clouds shape the instantaneous CO_2 forcing at the TOA. The radiative transfer model and the data set used here are described in Section 2. In Section 3, we focus on the causes of negative forcing under clear-sky conditions, which mainly occur in Antarctica. We quantify the

19448007, 2024, 1, Downloaded from https://agupubs.onlinelibrary.wiley.com/doi/10.1029/2023GL106433, Wiley Online Library on [16/01/2024]. See the Terms and Conditions (https://onlinelibrary.wiley.com/terms-and-conditions) on Wiley Online Library for rules of use; OA articles are governed by the applicable Creative Commons License

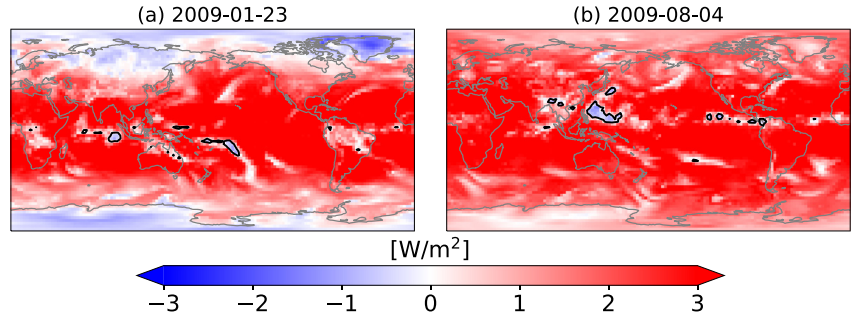

Figure 1. The daily mean forcing pattern of CO_2 doubling on (a) 23 Jan 2009, near the onset of a major mid-winter SSW event, and (b) 4 Aug 2009, when there are strong cloud masking effects in the western North Pacific from intensifying typhoon Morakot. The black contour shows longwave cloud radiative effect (CRE) of 120 Wm^{-2}.

forcing contributed by the near-surface temperature inversion and stratospheric inversion, with a novel approach that decomposes the forcing into bulk spectral regions, which feature different sensitivities to temperature structures. We also discuss why the negative CO_2 forcing is less common in the Arctic than in Antarctica. Section 4 discusses negative forcing under all-sky conditions. We also use idealized experiments, in which the temperature and clouds are modified to show how the temperature structure and clouds affect the sign of CO_2 forcing. We conclude in Section 5.

2. Radiative Transfer Calculation

We use standalone longwave Rapid Radiative Transfer Model (RRTMG, Mlawer et al., 1997), which calculates fluxes ranging from 10 to 3,250 cm^{-1}. The climatology of atmospheric profiles, including temperature, specific humidity, and ozone, are from ERA5 reanalysis data set of the European Centre for Medium-Range Weather Forecasts (Hersbach et al., 2020). The radiative forcing of doubled CO_2 is calculated as the flux difference between 760 and 380 ppmv CO_2 concentrations. The concentration of other well-mixed greenhouse gases, CH_4 and N_2O, are prescribed to 1.797 and 0.323 ppmv, respectively. CFCs are not included.

RRTMG performs the radiative transfer calculation at a total of 140 g-points, with each accounting for one monochromatic spectral node where the wavenumbers with similar absorption coefficients are grouped together beforehand. The fluxes at individual *g*-points are summed to get the bandwise and the broadband fluxes. This technique, named the correlated-*k* method (Fu & Liou, 1992), is a numerical treatment that speeds up computation (vs. calculating fluxes at a small, fixed wavenumber increment like line-by-line radiative transfer).

3. Negative CO_2 Forcing Under Clear-Sky Conditions

3.1. Temperature Modification Experiments

To evaluate the role of inversions on CO_2 forcing, we calculate the forcing with modified temperature soundings of the South Pole. Specifically, the near-surface inversion is removed by replacing the temperature below 500 hPa with temperature at the 500 hPa (smooth_Ts-T500), and the stratospheric inversion is removed by setting temperature above 30 hPa with temperature at the 30 hPa (smooth_T30up). In both experiments, we choose to leave T_{SFC} unperturbed because T_{SFC} determines the upward longwave emission, which is an important energetic constraint. How T_{SFC} itself affects the forcing will be briefly discussed at the end of this section. The water vapor in the polar regions is scarce and does not change the results qualitatively, so we keep using climatological water vapor profiles to highlight the role of temperature structure even if the near-surface layer might be supersaturated when the near-surface temperature is reduced.

Figures 2a and 2b plot the climatological temperature profile at the South Pole and the resulting instantaneous CO_2 forcing. Consistent with previous literature, the CO_2 forcing is found negative throughout September to March (Chen et al., 2023; Freese & Cronin, 2021; Schmithüsen et al., 2015; K. L. Smith et al., 2018). We note that December features the strongest negative forcing yet the near-surface inversion is the weakest. Surprisingly, despite large temperature reductions imposed in smooth_Ts-T500 experiment sometimes exceeding 20 K in the

19448007, 2024, 1, Downloaded from https://agupubs.onlinelibrary.wiley.com/doi/10.1029/2023GL106433, Wiley Online Library on [16/01/2024]. See the Terms and Conditions (https://onlinelibrary.wiley.com/terms-and-conditions) on Wiley Online Library for rules of use; OA articles are governed by the applicable Creative Commons License

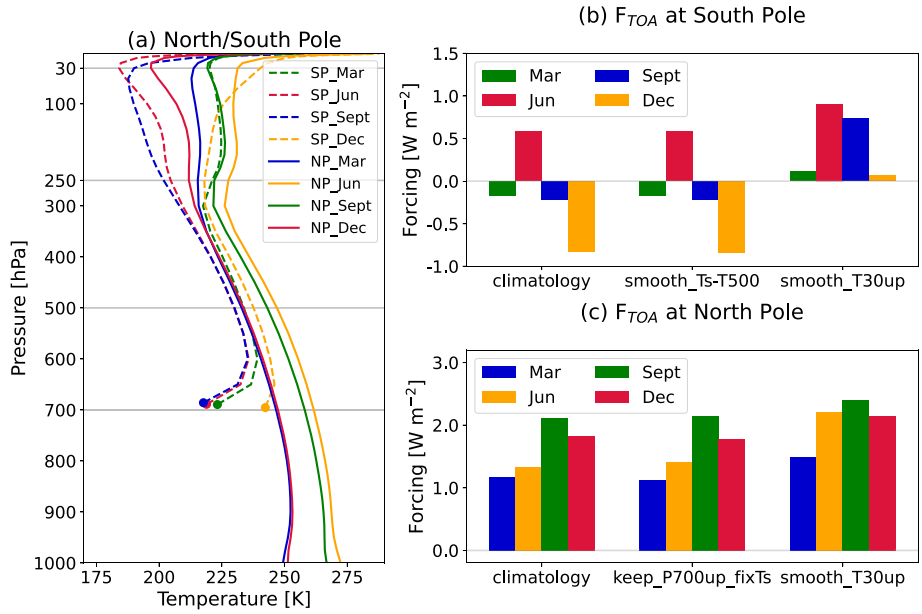

Figure 2. (a) The seasonality of climatological temperature at the South and North Pole. The pressure levels relevant to temperature modification experiments (30, 500, 700 hPa) and the tropopause (250 hPa) are plotted in gray horizontal lines for reference (see Sections 3.1 and 3.3 for details). (b) The broadband, instantaneous CO_2 forcing at the TOA based on the climatological profile and temperature modification experiments of the South Pole (Section 3.1). (c) Same as (b) but for the North Pole (Section 3.3). Note that the range of *y*-axis in (b) and (c) is different.

lower troposphere, the forcing changes by less than 0.01 Wm^{-2}. In contrast, the changes in the stratospheric lapse rate in smooth_T30up effectively eliminate the negative forcing and can increase the forcing by ∼1 Wm^{-2}. These suggest a dominant role of stratospheric temperature in modifying the CO_2 forcing, at least when T_{SFC} remains unchanged.

3.2. Attributing the Radiative Forcing to the Temperature Profile

According to Equation 1, the flux at the TOA comes from various altitudes of the atmosphere owing to the wavelength-varying $\tau_\nu(z)$ and $W_\nu(z)$ structure. In other words, one can relate the forcing and the contributing atmospheric level by calculating $W_\nu(z)$ in Equation 3 once $\tau_\nu(z)$ is known.

We exploit the spectral information in the model by outputting the optical depths and radiative fluxes at all 140 g-points, and regroup the *g*-point-based fluxes according to which part of the atmosphere the climatological emission layer [$\tau_g(z) = 1$] belongs to. The *g*-point-based fluxes are sorted into three groups with the following definitions:

- Stratosphere: *g*-points which $\tau_g(z_{250}) > 1$.
- Troposphere: *g*-points which $\tau_g(z_{250}) < 1$ and $\tau_g(z_{sfc}) > 1$.
- Window: *g*-points which $\tau_g(z_{sfc}) < 1$.

The subscript of z denotes the associated pressure level, and the tropopause is set at 250 hPa for convenience. In this definition, the first term on the RHS of Equation 1, the forcing coming from the surface, is mostly included in the window group. Together with Equation 3, the *g*-point grouped weighting function is calculated as:

$$W_i(z) = \frac{1}{I(0)} \sum_{g=0}^{n} I_g(0) \cdot \frac{dTr_g(z)}{dz}, \tag{6}$$

where the subscript g denotes the fluxes in the *g*-point dimension and the sum is over the *g*-points where the emission layer lies in the atmospheric layer group i defined above. Compared to using RRTMG's 16-band outputs that are segregated by respective gas absorption properties beforehand, this method offers a finer view of what part of the atmospheric profile contributes to the radiative fluxes.

19448007, 2024, 1, Downloaded from https://agupubs.onlinelibrary.wiley.com/doi/10.1029/2023GL106433, Wiley Online Library on [16/01/2024]. See the Terms and Conditions (https://onlinelibrary.wiley.com/terms-and-conditions) on Wiley Online Library for rules of use; OA articles are governed by the applicable Creative Commons License

19448007, 2024, 1, Downloaded from https://agupubs.onlinelibrary.wiley.com/doi/10.1029/2023GL106433, Wiley Online Library on [16/01/2024]. See the Terms and Conditions (https://onlinelibrary.wiley.com/terms-and-conditions) on Wiley Online Library for rules of use; OA articles are governed by the applicable Creative Commons License

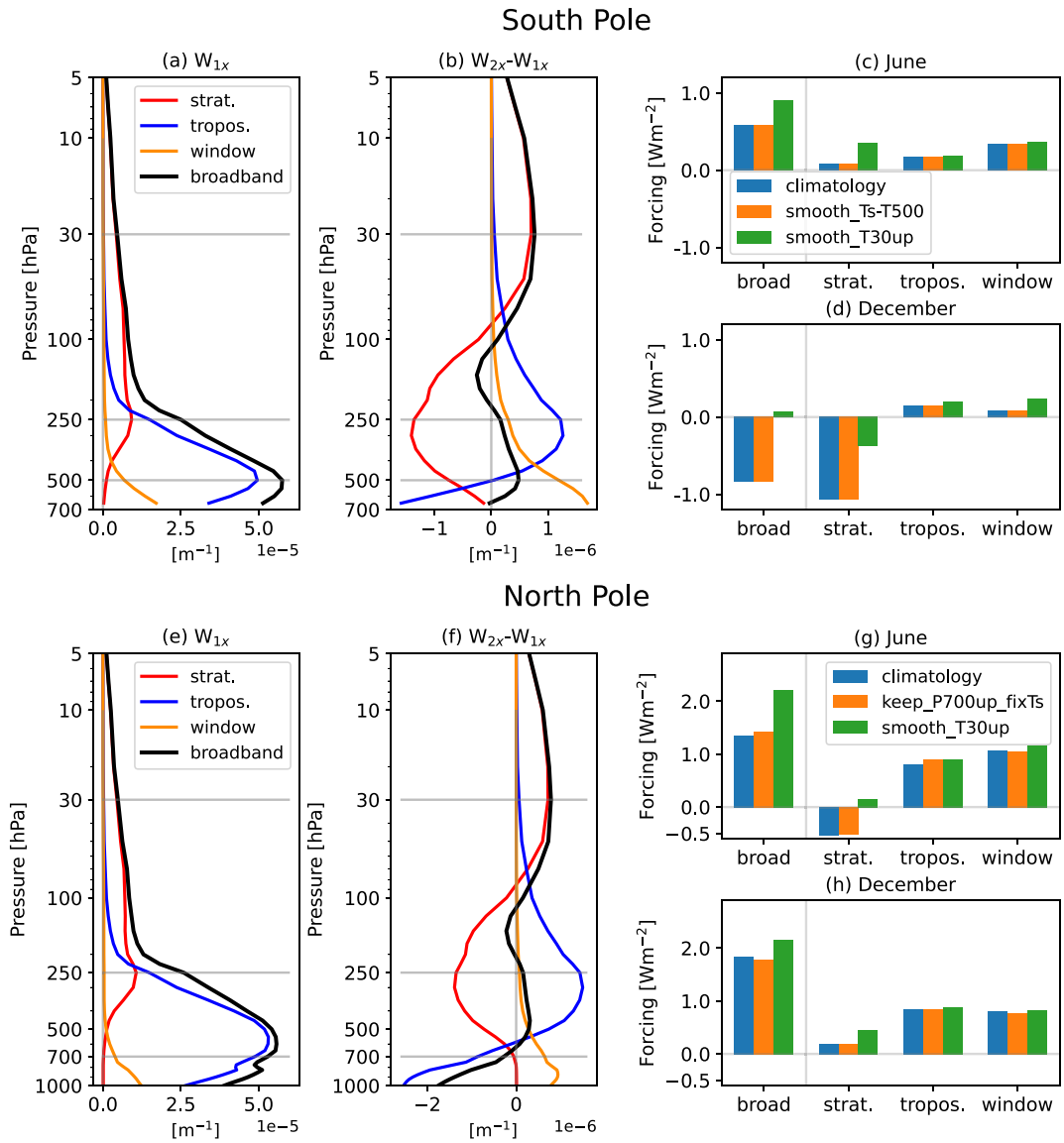

Figure 3. Forcing attribution based on optical depth grouping (introduced in Section 3.2) for Antarctica and the Arctic. (a) The grouped weighting function $W(z)$ [Equation 6] of annual-mean Antarctic climate with control CO_2 for absorption lines with emission layer in the stratosphere (red), troposphere (blue), and window (yellow). The broadband $W(z)$ (sum of all groups) is shown in black. (b) Same as (a) but for the change of $W(z)$ from CO_2 doubling. (c)–(d) The TOA forcing of $2 \times CO_2$ of temperature modification experiments for Antarctica sounding in June and December. (e)–(h) Same as (a)–(d) but for the Arctic. See Sections 3.1 and 3.3 for experiment design. The pressure levels relevant to temperature modification experiments (30, 500, 700 hPa) and the tropopause (250 hPa) are plotted in gray horizontal lines for reference.

Figure 3a presents the grouped $W(z)$ according to Equation 6: $W(z)$ in the stratosphere, troposphere, and window groups have a maximum of $W(z)$ in the associated pressure level, respectively. The broadband $W(z)$ depends on the total optical depth of all absorbing gases (e.g., H_2O, CO_2, and O_3) and has a peak at around 500 hPa, meaning that in Antarctica, most of the upwelling longwave at the TOA comes from around the lower troposphere with associated emission temperature. The change of $W(z)$ by CO_2 doubling is shown in Figure 3b. At first glance, an upward shift of the emission layer is clear in the stratosphere and troposphere groups: $\Delta W(z)$ of the stratosphere group is positive above 100 hPa and negative below, and $\Delta W(z)$ of the troposphere group is positive in the upper troposphere and negative in the lower troposphere. $\Delta W(z)$ of the window group is positive with a bottom-heavy structure, which implies increasing emissions from all levels with the largest increase near surface. This is because $\tau_g(z_{sfc})$ is smaller than unity in the window group so that the conventional definition of the emission layer

19448007, 2024, 1, Downloaded from https://agupubs.onlinelibrary.wiley.com/doi/10.1029/2023GL106433, Wiley Online Library on [16/01/2024]. See the Terms and Conditions (https://onlinelibrary.wiley.com/terms-and-conditions) on Wiley Online Library for rules of use; OA articles are governed by the applicable Creative Commons License

$\tau_g(z) = 1$ lies below the surface. Overall, there is a strong cancellation below 100 hPa across all groups. The major broadband $\Delta W(z)$ is in the stratosphere, which mainly comes from the g-points that comprise the 630–700 cm^{-1} band of RRTMG and implies that the forcing change due to the emission layer elevation within the stratosphere originates from the CO_2 band center.

Figures 3c and 3d show the decomposed forcing change of temperature modification experiments (Section 3.1) in $W(z)$ groups to evaluate the forcing sensitivity to the temperature structure. We only show the decomposed forcing of Antarctic summer (December) and winter (June), as the results in other seasons are qualitatively similar. Comparing the climatology and smooth_Ts-T500, the near-surface inversion has almost no effect: not only for the broadband forcing but also for the troposphere and window groups. This is because there is also a surface contribution due to non-zero $W(z)$ there, and the additional CO_2 increases ϵ_{ATM} [the integral of $W(z)$ with respect to height]. This ϵ_{ATM} increase slightly enhances the atmosphere's emission-to-space but also blocks emission from the surface by decreasing Tr(0). The combined contribution depends more on T_{SFC} but not the tropospheric inversions.

In contrast, smooth_T30up has an anomalous positive forcing in the stratosphere group. This is consistent with an upward shift of $W(z)$ into the modified colder stratosphere (less negative lapse rate) reducing OLR, which makes the forcing less negative or even positive. This also supports the argument that the emission temperature change owing to stratospheric temperature structure is key to a negative forcing. Aside from the stratosphere group, smooth_T30up increases the forcing from the troposphere and the window groups because $2 \times CO_2$ also increases their $\Delta W(z)$ in the stratosphere, though the change is an order smaller than in the near-surface. Additional sensitivity tests on varying aspects of stratospheric structure, like mean stratospheric temperature or the strength of inversion (not shown) confirm the inference from the shape of broadband $\Delta W(z)$ change (Figure 3b) that the "bulk" lapse rate between 150 and 10 hPa is key.

3.3. Forcing Asymmetry Between the Arctic and Antarctica

While the Arctic can have, at times, negative CO_2 forcing (Figure 1a), what accounts for the mean difference between polar regions? The Arctic forcing is overall 1–2 Wm^{-2} larger than Antarctica and is always positive for climatological conditions (Figure 2c). Figures 3e and 3f show that $\Delta W(z)$ above 700 hPa in the Arctic is similar to Antarctica, with a large broadband $\Delta W(z)$ in the stratosphere. A contrast here is that the broadband $\Delta W(z)$ turns negative below 700 hPa. We extend the temperature modification experiments to the Arctic. In addition to smooth_T30up, we quantify how the bottom 300 hPa air mass affects the forcing by truncating the sounding at 700 hPa (keep_P700up_fixTs), with T_{SFC} unchanged. Similar to Antarctica, smooth_T30up enhances forcing in all seasons, whereas keep_P700up_fixTs does not show obvious differences (Figure 2c).

The decomposed forcing in Figures 3g and 3h shows that the stratosphere group has weakly positive or negative forcing with the climatological profile. Smooth_T30up, which cools the stratosphere, increases the forcing by 0.3–0.8 Wm^{-2}. Surprisingly, keep_P700up_fixTs removes the negative $\Delta W(z)$ in the lower troposphere but barely changes the forcing. This results from the differences of base states under control CO_2: a thinner atmosphere is more transparent, and Tr(0) is more sensitive to CO_2 changes. Even though keep_P700up_fixTs seemingly excludes the positive forcing stemming from negative $\Delta W(z)$ in the bottom 300 hPa, a larger decrease in Tr(0) increases the forcing and the net effect is small. As the forcing from the troposphere and window groups are both larger than Antarctica by about 0.5–1 Wm^{-2}, a negative forcing in the Arctic requires an extraordinarily warm upper stratosphere to increase the inversion strength, like in a sudden stratospheric warming (Figure 1a).

While our results consistently indicate an important role of stratospheric temperature inversion for TOA forcing, a different approach to changing the tropospheric inversion and truncating the sounding might affect the interpretation. For example, Flanner et al. (2018) removed the inversion by increasing low-level temperature and T_{SFC} by up to 30 K and showed that the negative forcing vanishes. Yet, T_{SFC} increase essentially increases the surface contribution of the TOA forcing via the window band [first term of RHS in Equation 1]. This implicitly suggested negative forcing would be rare in the Arctic, as T_{SFC} there is ≈30 K warmer than Antarctica. If a lower T_{SFC} is used for Arctic truncation experiments (replacing T_{SFC} with T_{700}), the forcing will be reduced by 0.1–0.5 Wm^{-2} but is still positive (not shown).

4. Negative CO_2 Forcing Under All-Sky Conditions

Clouds are known to reduce the CO_2 forcing (Govindasamy & Caldeira, 2000). Here, we examine the role of clouds in reducing tropical forcing (Figure 1) and assess the role of stratosphere temperature structure in reducing the forcing, as was important for the clear-sky forcing in Antarctica.

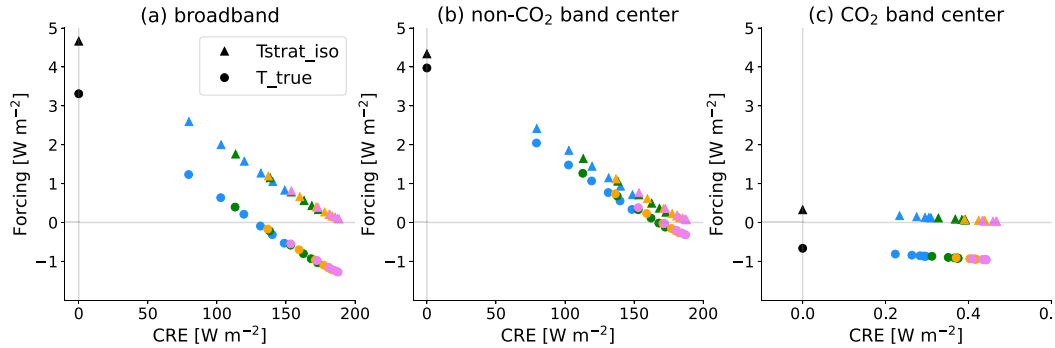

Figure 4. All-sky $2 \times CO_2$ forcing with a tropical-mean sounding (circles) and tropical-mean sounding but with isothermal stratosphere with cold point temperature above 100 hPa (triangles) for (a) broadband forcing, (b) non-CO_2 absorption band center (bands other than 630–700 cm^{-1}), and (c) CO_2 absorption band center (630–700 cm^{-1}). Color marks the cloud ice mixing ratio from less to more with blue to red. The horizontal axis is the CRE of the specified band. The black marker where the CRE equals zero is the clear-sky forcing.

We compute forcing with different clouds using a tropical-mean sounding. For simplicity, we employ single-layer slab clouds with 100% cloud fraction and the cloud ice mixing ratio ranges linearly from 1.5×10^{-5} to 4.5×10^{-5}. The cloud tops are fixed at the tropopause (100 hPa), with the cloud bottoms varying between 125 and 250 hPa. These parameters create a range of longwave CRE from 50 to 190 Wm^{-2}. To assess the role of the stratosphere, the all-sky forcing is computed with a similar sounding but with an isothermal stratosphere, where the stratospheric temperatures are fixed at the cold point temperature (100 hPa here), a common simplification in analytical radiative forcing/feedback analyses (Jeevanjee & Fueglistaler, 2020; Koll et al., 2023; Romps et al., 2022).

Figure 4a shows a linear dependence of broadband all-sky forcing on CRE. This is consistent with Chen et al. (2023) for the $2 \times CO_2$ forcing reduction by clouds with a linear regression model using longwave CRE as the predictor:

$$\Delta F_{cld} = -0.57 - 0.53\frac{\mathrm{CRE} - 20.06}{20.06}, \tag{7}$$

where ΔF_{cld} is the forcing difference under all-sky and clear-sky conditions. Interestingly, the forcing changes sign at 120 Wm^{-2}, which can be predicted by the regression model as the CRE required to zero 3.2 Wm^{-2} clear-sky forcing. An isothermal stratosphere barely changes CRE, and the forcing approaches but never goes below zero.

Since clouds feature strong, spectrally broad absorption, the refined *g*-point-based decomposition (Section 3.2) is gratuitous. We instead use RRTMG's built-in output bands for all-sky analyses. In the tropics, the stratosphere's role in forcing largely arises from the CO_2 absorption band center (630–700 cm^{-1}). This band dominates the forcing difference between the control and isothermal stratosphere (Figures 4b and 4c). This is slightly different from the polar regions, where the stratospheric emission extends to adjacent bands (500–630 and 700–820 cm^{-1}). Figure 4b further shows that the clouds impose strong masking effects in the non-CO_2 bands, consistent with expectations that clouds reduce forcing everywhere other than the stratosphere component. The negative forcing mainly comes from CO_2 band center (Figure 4c), where the emission is dominated by the stratosphere, and the forcing remains positive with an isothermal stratosphere. We conclude that the negative forcing under all-sky results from increased emission from the stratosphere in response to CO_2. As the positive forcing from the troposphere and the window are usually large in the tropics, negative forcing from the stratosphere wins only when the contribution below tropopause is greatly reduced by clouds with strong CRE.

5. Conclusion

This study explores the CO_2 forcing sensitivity to the vertical temperature structure, with an emphasis on what leads to a small, and even negative TOA forcing in the current climate. Two climate states with negative CO_2 forcing are discussed: the polar regions and the tropics. In brief, a negative forcing demands strong negative forcing from the stratosphere (enhanced emission-to-space mainly from CO_2 absorption band center near 660 cm^{-1}) and

19448007, 2024, 1, Downloaded from https://agupubs.onlinelibrary.wiley.com/doi/10.1029/2023GL106433, Wiley Online Library on [16/01/2024]. See the Terms and Conditions (https://onlinelibrary.wiley.com/terms-and-conditions) on Wiley Online Library for rules of use; OA articles are governed by the applicable Creative Commons License

19448007, 2024, 1, Downloaded from https://agupubs.onlinelibrary.wiley.com/doi/10.1029/2023GL106433, Wiley Online Library on [16/01/2024]. See the Terms and Conditions (https://onlinelibrary.wiley.com/terms-and-conditions) on Wiley Online Library for rules of use; OA articles are governed by the applicable Creative Commons License

relatively weak forcing from the combined contribution from the troposphere and window (mainly from other parts of the spectrum with where CO_2 is less absorbing). These two components depend on the stratospheric and near-surface temperature, respectively. These ingredients were viewed as important to a negative forcing in Schmithüsen et al. (2015) and K. L. Smith et al. (2018), although the physical picture of the two-level model they used is overly simplified. In polar climates, the effect of near-surface temperature structure is muted because the emission layer changes within the troposphere and the surface contribution counteract each other. The forcing is thus insensitive to the tropospheric temperature structure, at odds with the conventional argument that the near-surface inversion is key to negative forcing in Antarctica (Flanner et al., 2018; Sejas et al., 2018). In the tropics, there is abundant forcing coming from the troposphere and the window (i.e., away from the CO_2 absorption center). Therefore, a strong CRE is essential to mask the forcing stemming from the troposphere to enable the strong emission-to-space from the stratosphere to turn the broadband forcing negative.

Two major factors that make the current Antarctic climate a distinct region with negative CO_2 forcing include the low surface temperature, which reduces positive forcing, and the high stratospheric temperature, which enhances negative forcing. Both factors are less extreme in the Arctic climate. There are still rare occasions when there is negative CO_2 forcing in the Arctic, such as during strong sudden stratospheric warming events when the stratosphere warms by tens of K (e.g., Baldwin et al., 2021). We also note that the relative importance between surface and stratospheric temperature may depend on CO_2 concentrations. For example, under higher base CO_2 concentration, the instantaneous TOA forcing is more sensitive to the emission layer changes in the stratosphere, whereas the troposphere and surface temperature may have more weight for a very low CO_2 scenario. These may lead to a non-monotonically forcing dependence on CO_2 concentration (e.g., Figure 1a of Freese & Cronin, 2021).

By examining the cause of negative CO_2 forcing, this study highlights the stratosphere's role in shaping the TOA forcing. It also demonstrates the value of resolving the spectral dimension of radiation. Simple gray-radiation, broadband optical depth perspectives (e.g., Equation 5) that do not identify spectral emission characteristics would lead to inaccurate radiation sensitivity to either surface or stratospheric temperature. Other greenhouse gases (e.g., CH_4) with less strong absorption band centers may behave differently because of smaller $\Delta W(z)$ in the stratosphere, an interesting area for future research. Meanwhile, a greenhouse gas perturbation with a vertical structure, such as an isolated near-surface CFC increase (Flanner et al., 2018), would mainly modify emission from layers adjacent to perturbations. This could result in interpretations that differ from those of a well-mixed greenhouse gas perturbation as used in this study.

Our analysis here focuses on the spectral competition that can give rise to negative TOA forcing, though this competition is also relevant to small-but-positive forcing. We also reiterate that negative TOA forcing does not imply that additional CO_2 cools the surface, as adjustments are important to the re-establishment of Antarctica's energy balance (Myhre et al., 2013; K. L. Smith et al., 2018). The vertically-decomposed forcing revealed by our spectral analyses, instead, could be quantitatively helpful in understanding why the forcings of different greenhouse gases vary in their stratospheric and tropospheric temperature adjustments (C. J. Smith et al., 2018, 2020). The interplay between the vertical forcing variation of a particular forcing agent and the accompanying adjustments warrants further investigation.

Data Availability Statement

The scripts to generate data and figures are available at Chen (2023).

Acknowledgments
We acknowledge the supports of the Natural Sciences and Engineering Research Council of Canada (RGPIN-2019-04511), Fonds de Recherche Nature et Technologies of Quebec (2021-PR-283823), and the Cooperative Institute for Modeling Earth Systems under award NA18OAR4320123 from the National Oceanic and Atmospheric Administration, U.S. Department of Commerce. YTC acknowledges the supports of Stephen and Anastasia Mysak Fellowship of McGill University.

References

Baldwin, M. P., Ayarzagüena, B., Birner, T., Butchart, N., Butler, A. H., Charlton-Perez, A. J., et al. (2021). Sudden stratospheric warmings. *Reviews of Geophysics*, *59*(1), e2020RG000708. https://doi.org/10.1029/2020RG000708

Chen, Y.-T. (2023). The cause of negative CO_2 forcing at the top-of-atmosphere: The role of stratospheric vs. tropospheric temperature inversions [Software]. Zenodo. https://doi.org/10.5281/zenodo.10064826

Chen, Y.-T., Huang, Y., & Merlis, T. M. (2023). The global patterns of instantaneous CO_2 forcing at the top of the atmosphere and the surface. *Journal of Climate*, *36*(18), 6331–6347. https://doi.org/10.1175/JCLI-D-22-0708.1

Flanner, M. G., Huang, X., Chen, X., & Krinner, G. (2018). Climate response to negative greenhouse gas radiative forcing in polar winter. *Geophysical Research Letters*, *45*(4), 1997–2004. https://doi.org/10.1002/2017gl076668

Freese, L. M., & Cronin, T. W. (2021). Antarctic radiative and temperature responses to a doubling of CO_2. *Geophysical Research Letters*, *48*(17), e2021GL093676. https://doi.org/10.1029/2021gl093676

Fu, Q., & Liou, K. N. (1992). On the correlated k-distribution method for radiative transfer in nonhomogeneous atmospheres. *Journal of the Atmospheric Sciences*, *49*(22), 2139–2156. https://doi.org/10.1175/1520-0469(1992)049<2139:otcdmf>2.0.co;2

Govindasamy, B., & Caldeira, K. (2000). Geoengineering Earth's radiation balance to mitigate CO_2-induced climate change. *Geophysical Research Letters*, *27*(14), 2141–2144. https://doi.org/10.1029/1999gl006086

Hersbach, H., Bell, B., Berrisford, P., Hirahara, S., Horányi, A., Muñoz-Sabater, J., et al., (2020). The ERA5 global reanalysis. *Quarterly Journal of the Royal Meteorological Society*, *146*(730), 1999–2049. https://doi.org/10.1002/qj.3803

Huang, Y., & Bani Shahabadi, M. (2014). Why logarithmic? A note on the dependence of radiative forcing on gas concentration. *Journal of Geophysical Research: Atmospheres*, *119*(24), 13683–13689. https://doi.org/10.1002/2014jd022466

Huang, Y., Tan, X., & Xia, Y. (2016). Inhomogeneous radiative forcing of homogeneous greenhouse gases. *Journal of Geophysical Research*, *121*(6), 2780–2789. https://doi.org/10.1002/2015jd024569

Jeevanjee, N., & Fueglistaler, S. (2020). On the cooling-to-space approximation. *Journal of the Atmospheric Sciences*, *77*(2), 465–478. https://doi.org/10.1175/JAS-D-18-0352.1

Jeevanjee, N., Seeley, J., Paynter, D., & Fueglistaler, S. (2021). An analytical model for spatially varying clear-sky CO_2 forcing. *Journal of Climate*, *34*(23), 9463–9480.

Koll, D. D. B., Jeevanjee, N., & Lutsko, N. J. (2023). An analytic model for the clear-sky longwave feedback. *Journal of the Atmospheric Sciences*, *80*(8), 1923–1951. https://doi.org/10.1175/JAS-D-22-0178.1

Mlawer, E. J., Taubman, S. J., Brown, P. D., Iacono, M. J., & Clough, S. A. (1997). Radiative transfer for inhomogeneous atmospheres: RRTM, a validated correlated-k model for the longwave. *Journal of Geophysical Research*, *102*(D14), 16663–16682. https://doi.org/10.1029/97JD00237

Myhre, G., Shindell, D., Bréon, F.-M., Samset, B. H., Hodnebrog, Sillmann, J., et al. (2013). Anthropogenic and natural radiative forcing. In T. F. Stocker, et al. (Eds.), *Climate change 2013: The physical science basis* (pp. 659–740). Cambridge University Press.

Romps, D. M., Seeley, J. T., & Edman, J. P. (2022). Why the forcing from carbon dioxide scales as the logarithm of its concentration. *Journal of Climate*, *35*(13), 4027–4047. https://doi.org/10.1175/jcli-d-21-0275.1

Schmithüsen, H., Notholt, J., König-Langlo, G., Lemke, P., & Jung, T. (2015). How increasing CO_2 leads to an increased negative greenhouse effect in Antarctica. *Geophysical Research Letters*, *42*(23), 10422–10428. https://doi.org/10.1002/2015gl066749

Sejas, S. A., Taylor, P. C., & Cai, M. (2018). Unmasking the negative greenhouse effect over the Antarctic Plateau. *Npj Climate and Atmospheric Science*, *1*(17), 2397–3722.

Smith, C. J., Kramer, R. J., Myhre, G., Alterskjær, K., Collins, W., Sima, A., et al. (2020). Effective radiative forcing and adjustments in CMIP6 models. *Atmospheric Chemistry and Physics*, *20*(16), 9591–9618. https://doi.org/10.5194/acp-20-9591-2020

Smith, C. J., Kramer, R. J., Myhre, G., Forster, P. M., Soden, B. J., Andrews, T., et al. (2018a). Understanding rapid adjustments to diverse forcing agents. *Geophysical Research Letters*, *45*(21), 12023–12031. https://doi.org/10.1029/2018GL079826

Smith, K. L., Chiodo, G., Previdi, M., & Polvani, L. M. (2018b). No surface cooling over Antarctica from the negative greenhouse effect associated with instantaneous quadrupling of CO_2 concentrations. *Journal of Climate*, *31*(1), 317–323. https://doi.org/10.1175/JCLI-D-17-0418.1

Zhang, M., & Huang, Y. (2014). Radiative forcing of quadrupling CO_2. *Journal of Climate*, *27*(7), 2496–2508. https://doi.org/10.1175/jcli-d-13-00535.1

19448007, 2024, 1, Downloaded from https://agupubs.onlinelibrary.wiley.com/doi/10.1029/2023GL106433, Wiley Online Library on [16/01/2024]. See the Terms and Conditions (https://onlinelibrary.wiley.com/terms-and-conditions) on Wiley Online Library for rules of use; OA articles are governed by the applicable Creative Commons License